J. Phys. Chem. A **2008,** *112,* 4853–4860

Molecular Structure of the *trans* and *cis* Isomers of Metal-Free Phthalocyanine Studied by Gas-Phase Electron Diffraction and High-Level Quantum Chemical Calculations: NH Tautomerization and Calculated Vibrational Frequencies

Tatyana Strenalyuk, Svein Samdal,* and Hans Vidar Volden

Centre for Theoretical and Computational Chemistry (CTCC), Department of Chemistry, University of Oslo, P.O. Box 1033 Blindern, NO-0315 Oslo, Norway

Received: February 13, 2008; Revised Manuscript Received: March 13, 2008

The molecular structure of the *trans* isomer of metal-free phthalocyanine (H_2Pc) is determined using the gas electron diffraction (GED) method and high-level quantum chemical calculations. B3LYP calculations employing the basis sets 6-31G**, 6-311++G**, and cc-pVTZ give two tautomeric isomers for the inner H atoms, a *trans* isomer having D_{2h} symmetry and a *cis* isomer having C_{2v} symmetry. The *trans* isomer is calculated to be 41.6 (B3LYP/6-311++G**, zero-point corrected) and 37.3 kJ/mol (B3LYP/cc-pVTZ, not zero-point corrected) more stable than the *cis* isomer. However, Hartree−Fock (HF) calculations using different basis sets predict that *cis* is preferred and that *trans* does not exist as a stable form of the molecule. The equilibrium composition in the gas phase at 471 °C (the temperature of the GED experiment) calculated at the B3LYP/6-311++G** level is 99.8% *trans* and 0.2% *cis*. This is in very good agreement with the GED data, which indicate that the mole fraction of the *cis* isomer is close to zero. The transition states for two mechanisms of the NH tautomerization have been characterized. A concerted mechanism where the two H atoms move simultaneously yields a transition state of D_{2h} symmetry and an energy barrier of 95.8 kJ/mol. A two-step mechanism where a *trans* isomer is converted to a *cis* isomer, which is converted into another *trans* isomer, proceeds via two transition states of C_s symmetry and an energy barrier of 64.2 kJ/mol according to the B3LYP/6-311++G** calculation. The molecular geometry determined from GED is in very good agreement with the geometry obtained from the quantum chemical calculations. Vibrational frequencies, IR, and Raman intensities have been calculated using B3LYP/6-311++G**. These calculations indicate that the molecule is rather flexible with six vibrational frequencies in the range of 20−84 cm^{-1} for the *trans* isomer. The *cis* isomer might be detected by infrared matrix spectroscopy since the N−H stretching frequencies are very different for the two isomers.

Introduction

Metal phthalocyanines (MPcs) represent a class of molecules that attracts great attention in several different fields of science and industry. Their high thermal and chemical stability have made them suitable for many technological applications such as dyes, pigments, semiconductors, energy conversion in photovoltaic and solar cells, photosensitizers, electrophotography, molecular electronics, gas sensors, electrochromism in display devices, liquid crystals, Langmuir−Blodgett films, nonlinear optics, electrocatalytic reagents, and photodynamic therapy. Because of the similarity in structure to biologically important molecules such as chlorophyll and hemoglobin, they have attracted special interest. There are several excellent books about MPcs where the above-mentioned properties and applications are discussed.[1–6]

Since the first structural report on metal-free phthalocyanine (H_2Pc) in the solid state[7] was published in 1936, there have been several investigations, and a comprehensive summary is given by Engel.[4] H_2Pc exists in two different crystalline modifications, α and β, where the β modification is the most stable. Both the α modification[8,9] and the β modification[10–12] have been characterized by single-crystal X-ray diffraction. The main difference between the two modifications is the stacking of the individual molecules in the crystal. There is also a χ modification, which has not been characterized by single-crystal X-ray diffraction, but experimental data are available from various scattering techniques.[13] It has been difficult to locate the two inner H atoms by both X-ray[8,9,11,13] and neutron diffraction.[10] The Fourier map shows four peaks in front of the N isoindole atoms, and in this disorder, half of a H atom is bonded to each N isoindole atom. The nature of this disorder has been discussed, whether it is static or dynamic.[9,14] In the static model, the inner H atoms are ordered in the molecule, but the molecules in the crystal are randomly distributed with different orientations, while in the dynamic model, the H atoms jump between diagonal N sites. However, in the latest X-ray investigation of β-H_2Pc by Matsumoto et al.,[12] the two inner H atoms are located at diagonal N sites defined as the *trans* isomer; see Figure 1.

Quantum chemical calculations predict that metal-free porphyrin (H_2P) also exits as *cis* and *trans* isomers. The *trans* isomer is the most stable isomer. The inner H atoms migrate in a framework of the four N sites, and this double H atom transfer process is known as the NH tautomerization. This NH tautomerization has recently been reviewed.[15] The structures and the stability of *cis* and *trans* H_2P have been investigated by different theoretical and experimental methods. Spin-restricted

---

* To whom correspondence should be addressed. Tel: 47 2285 5458. Fax: +47 2285 5441. E-mail: svein.samdal@kjemi.uio.no.

10.1021/jp801284c CCC: $40.75

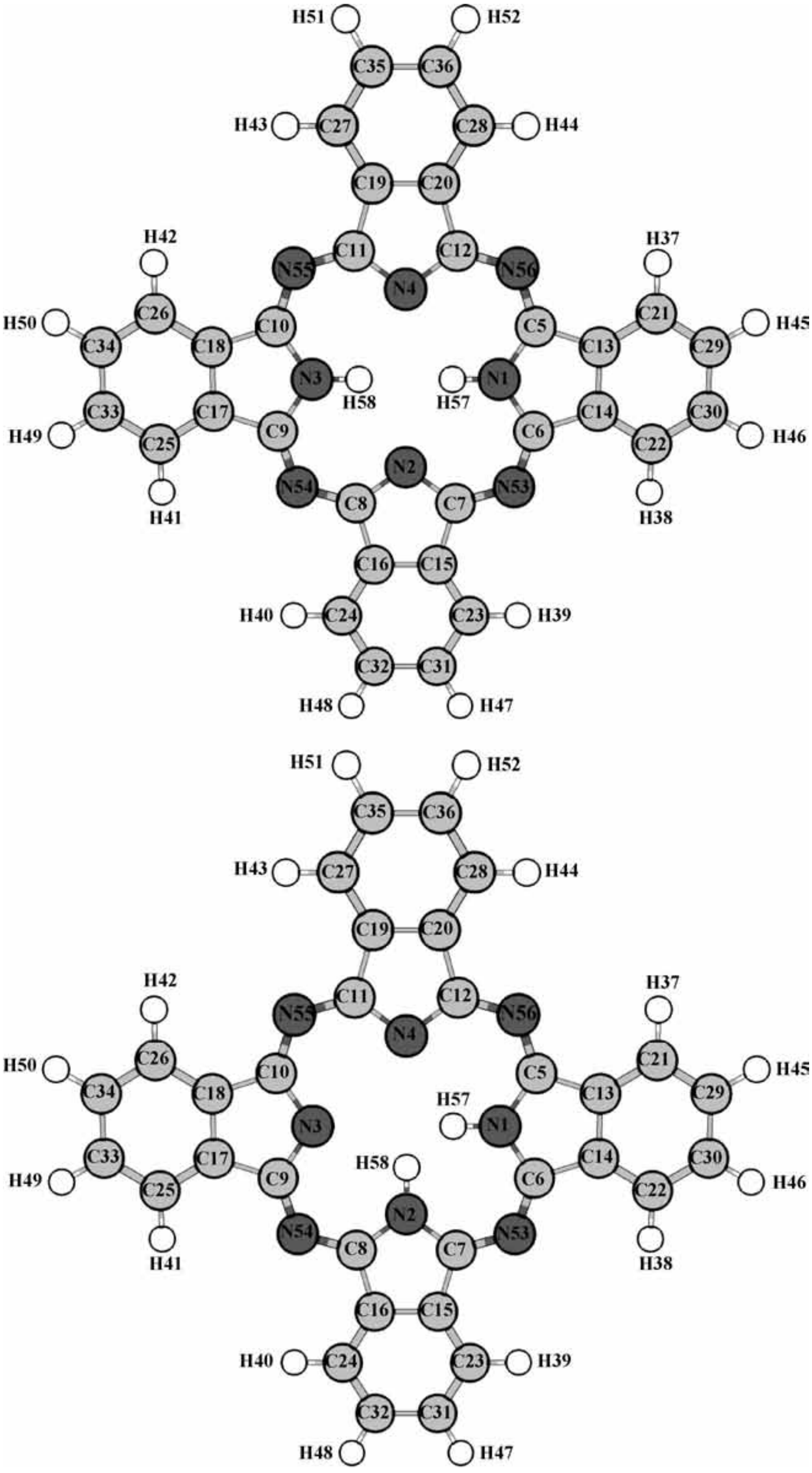

Figure 1. Molecular numbering of *cis* (below) and *trans* (above) isomers of H_2Pc.

calculations at the HF level are not able to give the correct geometry due to lack of inclusion of electron correlation effects.[16]

It should therefore be of interest to investigate whether H_2Pc behaves in the same way as H_2P. There is very little experimental information about the molecular structures of MPcs in the gas phase, but we have recently successfully investigated chlorododecafluorosubphthalocyanato boron(III) [SubPc(F)],[17] phthalocyanatozinc [ZnPc(H)], and hexadecafluorophthalocyanatozinc [ZnPc(F)].[18] A natural extension would be to investigate H_2Pc since this molecule is the prototype of the MPcs series of molecules, and its geometry should serve as reference geometry for other MPcs. This is the motivation for our investigation, and we will later extend our study to MPcs and similar systems using GED and high-level quantum chemical calculations. Hopefully, this will bring new and useful knowledge about this important class of molecules, which have so many technological applications. In this paper, we present our

TABLE 1: Experimental Conditions for H_2Pc

nozzle-to-plate distance (mm)	498.77	249.07
electron wavelength (pm)	5.82	5.82
nozzle temperature (°C)	471	471
s ranges (nm^{-1})		
x-direction	17.50−152.50	35.00−302.50
y-direction	17.50−122.50	35.00−248.75
Δs (nm^{-1})	1.25	1.25
number of plates	8	8
degree of polynomial[a]	8	10

[a] Degree of polynomial used in the background subtraction.

results from GED and high-level quantum chemical calculations on H_2Pc with molecular formula $C_{32}H_{18}N_8$, systematic name 29*H*,31*H*-phthalocyanine, and trivial name phthalocyanine.

Experimental Section

H_2Pc was obtained from Aldrich and used without further purification. The GED data were recorded on the Balzers KD-G2 unit at the University of Oslo, and the experimental setup was the same as for ZnPc(H) and ZnPc(F).[18] The experimental conditions are summarized in Table 1.

Quantum Chemical Calculations. The quantum chemical calculations were performed with the GAUSSIAN03 program package[19] running at the HP superdome facilities in Oslo. Several quantum chemical calculations[20–24] using different methods and basis sets as large as 6-31G** have been made for H_2Pc. B3LYP[25,26] has been widely used in theoretical studies of pyrrole macrocycles.[27–37] Our quantum chemical calculations on SubPc(F), ZnPc(H), and ZnPc(F) with different methods and basis sets confirm that B3LYP gives good agreement with the experimental results,[17,18] and it is expected that the B3LYP calculations would give good results for H_2Pc as well.

The basis sets that we have used are 6-31G**,[38] 6-311++G**,[39,40] and cc-pVTZ.[41] To our knowledge, the present calculations represent the highest level performed so far on H_2Pc. The numbering of the atoms for the *trans* and *cis* isomers is shown in Figure 1. The most important calculated structure parameters are given as Supporting Information (Tables S1 and S2 and energies as a footnote to Table S1).

Molecular force field calculations were made to ensure that the stationary points represent true minima, except for the cc-pVTZ basis set, which requires too much computer time. The reliability of the IR and Raman intensities is improved by introduction of diffuse and polarization functions.[42–45] Calculated frequencies and IR and Raman intensities using B3LYP/6-311++G** are given as Supporting Information (Table S3).

Electron Diffraction. A brief description of the electron diffraction method is given in a recent article on a related molecule SubPc(F).[17] This article may help in evaluating the experimental data, the strategies chosen for least-squares refinement, and the precision and accuracy of the structure parameters.

Structure Analysis. ***Model and Constraints.*** H_2Pc is the simplest phthalocyanine molecule. It consists of four isoindole subunits linked by azamethine bridges through the atoms N53, N54, N55, and N56. The two inner H atoms are small enough to be accommodated into the central cavity formed by the four isoindole N atoms N1, N2, N3, and N4. The numbering of the atoms is given on Figure 1.

The highest symmetry of the *trans* isomer is D_{2h}, where the two inner H atoms are attached to diagonally opposed isoindole N atoms. For the *trans* isomer, there are two molecular symmetry axes, one through the atoms N1 and N3 and another through the atoms N2 and N4. This gives two nonequivalent isoindole subunits, (H57, N1, C5, C6, C13, C14, C21, C22, C29, C30, H37, H38, H45, and H46) and (N2, C7, C8, C15, C16, C23, C24, C31, C32, H39, H40, H47, and H48).

The following parameters were chosen as independent parameters to describe the molecular geometry (distances): N1···N3, N2···N4, N1−H57, C21−H37, N1−C5, C5−C13, C13−C14, and (angles) C5−N1−C6, N1−C5−N56, C13−C14−C22, C13−C21−H37, and N1−C5−N56. Because the molecule is planar, all dihedral angles are either 180.0 or 0.0°.

According to the quantum chemical calculations, the differences between chemically similar bond distances and valence angles in the two nonequivalent subunits are too small to be determined with meaningful accuracy by the GED method. Therefore, introduced was the following set of constraints: (C13−C21) = (C13−C14) + Δ1, (C21−C29) = (C13−C14) + Δ2, (C29−C30) = (C13−C14) + Δ3, (C29−H45) = (C21−H37) + Δ4, (C15−C23−H39) = (C13−C21−H37) + Δ5, (N2−C7) = (N1−C5) + Δ6, (C7−N2−C8) = (C5−N1−C6) + Δ7, (C23−C31−H47) = (C13−C21−H37) + Δ8, (C7−C15) = (C5−C13) + Δ9, (C15−C16) = (C13−C14) + Δ10, (C21−C29−H45) = (C13−C21−H37) + Δ11, (C15−C23) = (C13−C14) + Δ12, (C16−C15−C23) = (C13−C14−C22) + Δ13, (C23−C31) = (C13−C14) + Δ14, (C31−C32) = (C13−C14) + Δ15, (C23−H39) = (C21−H37) + Δ16, (C31−H47) = (C21−H37) + Δ17, and (N5−N56) = (N1−C5) + Δ18. All differences, Δ1−Δ18, were taken from the molecular geometry optimized at the B3LYP/6-311++G** level, and they are −1.57 pm, −2.26 pm, −0.33 pm, 0.11 pm, 0.34°, −1.37 pm, −5.32°, −0.91°, 1.44 pm, −0.91 pm, −0.93°, −2.04 pm, 0.26°, −1.68 pm, −0.83 pm, 0.03 pm, 0.13 pm, and −6.16 pm, respectively. All Δ values could in principle be refined, and several attempts were made to determine some of them, but only Δ18 was successfully determined and added to the final set of variables.

Vibrational Corrections. The root-mean-squares amplitudes of vibration, u values, and perpendicular correction coefficients, k values, used for shrinkage correction in the GED analysis were calculated from the B3LYP/6-311++G** force fields using the SHRINK[46,47] program. The SHRINK program calculates these parameters using two different approaches. One approach is based on a rectilinear[48,49] movement of the atoms, and the other is based on a curvilinear[46,47] movement of the atoms. The latter approach is generally considered to be the more realistic, and this has been used in this investigation. The u_{h1} values from the curvilinear approach were refined in groups. The KCED25[50] least-squares fitting program was used to obtain structure parameters. The $r_e - r_a$ correction term, which is the difference between the bond length determined by GED (r_a) and quantum chemical calculations (r_e), is also estimated by the SHRINK program, and these differences are included in the final results given in Table 2.

Results and Discussion

Quantum Chemical Calculations. Previous investigations on metal-free phorphyrin (H_2P) revealed that HF calculations were not able to detect the *trans* isomer but only the *cis* isomer due to lack of inclusion of electron correlation.[16] This has also been tested on H_2Pc, and as for H_2P, only the *cis* isomer is found in HF 6-31G** and 6-311++G** calculations and confirmed by force field calculations. All quantum chemical B3LYP calculations predict that H_2Pc exists in two stable isomers, a *trans* isomer having D_{2h} symmetry, and a *cis* isomer having C_{2v} symmetry. MP2(FC)/6-31G* has been used to optimize the geometry for the *trans* and *cis* isomers, but force

TABLE 2: Experimental Results and Quantum Chemical Calculation for the *trans* Isomer of H_2Pc

parameter	r_e(GED)[a]	$r_e - r_a$	u_{exp}	u_{h1}[b]	k_{h1}[b]	DFT[d] r_e	neutr. diff.[g][10]	X-ray[8](α)[g]	X-ray[9] (α)[g]	X-ray[11] (β)[g]	X-ray[13] (β)[g]	X-ray[12] (β)[g]
						interatomic distances (pm)						
N1···N3	403.7(34)	−0.13	11.8(7)	12.5	1.748	404.7			392.3		395.5	395.3
N2···N4	384.3(36)	1.77	13.0	13.0	2.143	389.9			391.0		393.7	391.0
N1−H57	99.7[e]	−1.52	6.3(8)	7.1	0.143	101.2	94		84.1		90	92
C21−H37	109.4(8)	−1.59	6.7(8)	7.6	0.080	108.3	108	99.6	93.0	99.1	99	95
N1−C5	137.6(7)	−0.33	5.7(3)	5.3	0.036	137.7	137	137.4	137.6	137.4	136.7	137.3
C5−N56	133.6(17)[c]	−0.69	5.2(3)	4.7	−0.070	131.5	132	132.6	132.6	132.5	132.4	132.5
C5−C13	145.0(7)	−0.49	5.9(3)	5.4	0.025	145.2	147	144.9	145.9	145.5	145.7	145.3
C13−C14	141.6(5)	−0.22	5.6(3)	5.0	0.092	141.2	141	139.5	139.4	139.8	139.2	139.8
						bond angles (degrees)						
C5−N1−C6	110.9(7)					112.5	109	108.8	108.5	108.8	109.5	109.8
N1−C5−N56	127.2(8)					128.1	128	127.6	127.9	128.0	128.3	128.3
C13−C14−C22	121.2(2)					121.0	121	121.0	121.2	121.3	121.2	121.1
C13−C21−H37	120.5[e]					120.5	121	122.8	121.2	123.1	121.7	121.3
R_f[f] (%)	4.33											

[a] Parenthesized values are estimated error limits defined as $2.5[\sigma_{lsq}^2 + (0.001r)^2]^{1/2}$ for distances and $2.5\sigma_{lsq}$ for angles and amplitudes, where σ_{lsq} is one standard deviation taken from the least-squares refinements and $0.001r$ is 0.1% uncertainty in the electron wavelength. The errors are in the units of the last digits. [b] Curvilinear treatment of the vibrating atoms. [c] This value was calculated by using constraints between parameters. [d] B3LYP/cc-pVTZ. [e] This value was fixed to its B3LYP/cc-pVTZ value. [f] $R_f = [\sum s\, w(I_s^{obs} - I_s^{calcd})^2]/[\sum s\, w(I_s^{obs})^2] \times 100\%$, where w is a weight function usually equal to 1 and I is the molecular modified intensity. [g] Average values.

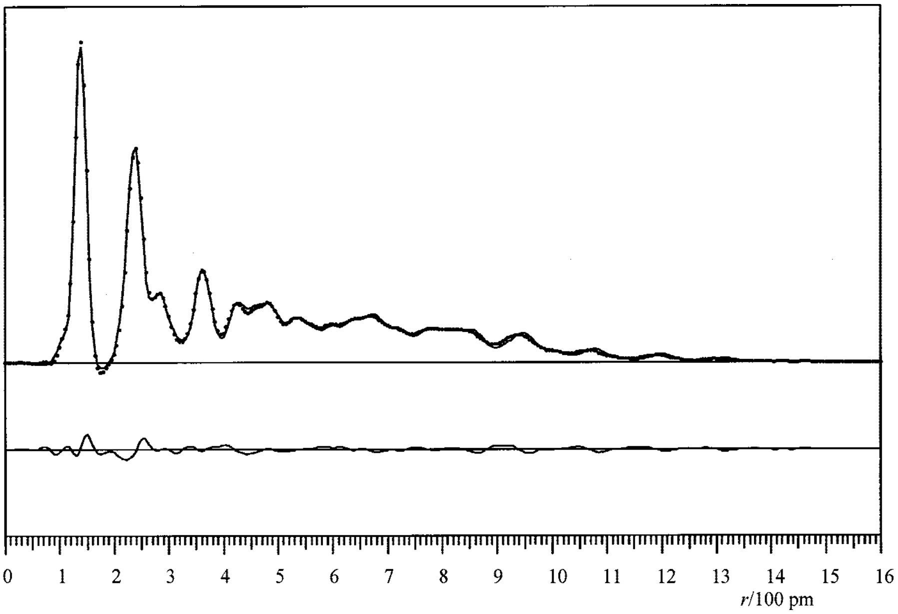

Figure 2. RD curves for the B3LYP/6-311++G** calculated *trans* isomer of H_2Pc. The experimental points (dots) are the average of the four curves shown in Figure 5, and theoretical points were used for the unobserved region $s < 17.50$ nm^{-1}. The damping coefficient for the RD function is 35 pm^2.The curve below is the difference curve. $R_f = 9.89\%$.

field calculations were too time consuming to verify that these forms represent energy minima.

The *trans* isomer is 41.6 (B3LYP/6-311++G**, zero point corrected) and 37.3 kJ/mol (B3LYP/cc-pVTZ, not zero-point corrected), respectively, more stable than the *cis* isomer. The most important bond distances and bond angles are given as Supporting Information (Tables S1 and S2 and energies in the footnote to Table S1). It can be seen from these two tables that there are very small differences between the bond lengths and the bond angles for the two stable isomers except for the bond angles related to the azamethine N atoms. This justifies the constraints that had to be made in the GED analysis.

NH Tautomerization. The two inner H atoms migrate in a framework of the four isoindole N atom sites. This double H atom transfer process is known as NH tautomerization, and a review of this process for H_2P is given by Maity and Truong.[15] There are two proposed mechanisms for the NH tautomerization process, a stepwise and a concerted. In the stepwise mechanism, the two H atoms migrate one after another from the *trans* (D_{2h}, N1−H, N3−H) through a transition state TS (C_s, N1−H, N2···H) to *cis* (C_{2v}, N1−H, N2−H) and a transition state TS (C_s, N4···H, N2−H) to *trans* (D_{2h}, N4−H, N2−H). The concerted mechanism involves synchronous migration of the two H atoms from *trans* (D_{2h}, N1−H, N3−H) to a transition state TS (C_{2h}, N4···H, N2···H) and *trans* (D_{2h}, N4−H, N2−H). For H_2P, it is both theoretically and experimentally proven that the double proton transfer occurs via a two-step mechanism rather than by a synchronous one-step mechanism.[15] The transition state specified as TS (C_s, N1−H, N2···H) is characterized by one N−H bond, and the other H atom is shared almost equally between two other N atoms (one intramolecular H-bonding) and corresponds to the stepwise mechanism; see Supporting Information Tables S1 and S2 for the complete geometry. The transition state specified as TS (C_{2h}, N4···H, N2···H) is characterized by no N−H bond, but where the two H atoms are equally shared between two N atoms (two

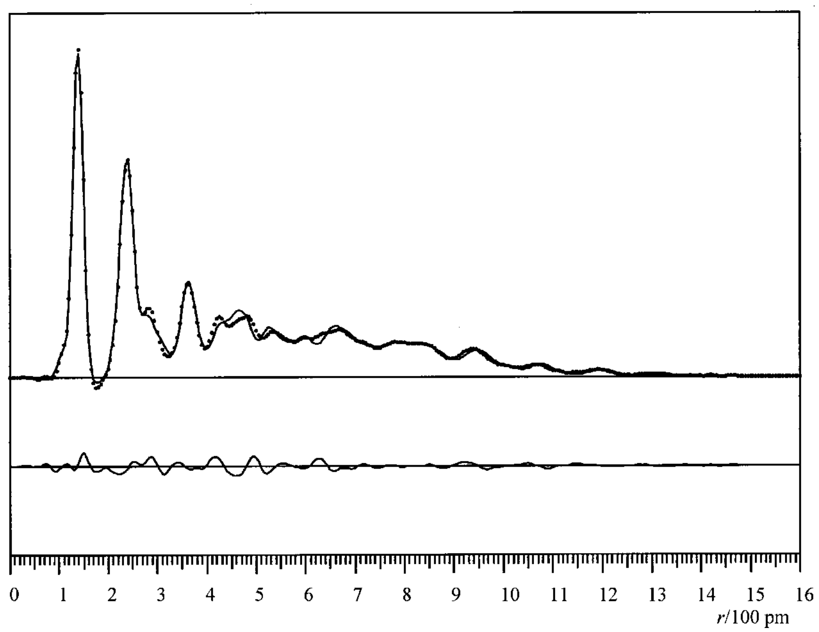

Figure 3. RD curves for the B3LYP/6-311++G** calculated *cis* isomer of H_2Pc. The experimental points (dots) are the average of the four curves shown in Figure 5, and theoretical points were used for the unobserved region $s < 17.50$ nm^{-1}. The damping coefficient for the RD function is 35 pm^2. The curve below is the difference curve. $R_f = 10.98\%$.

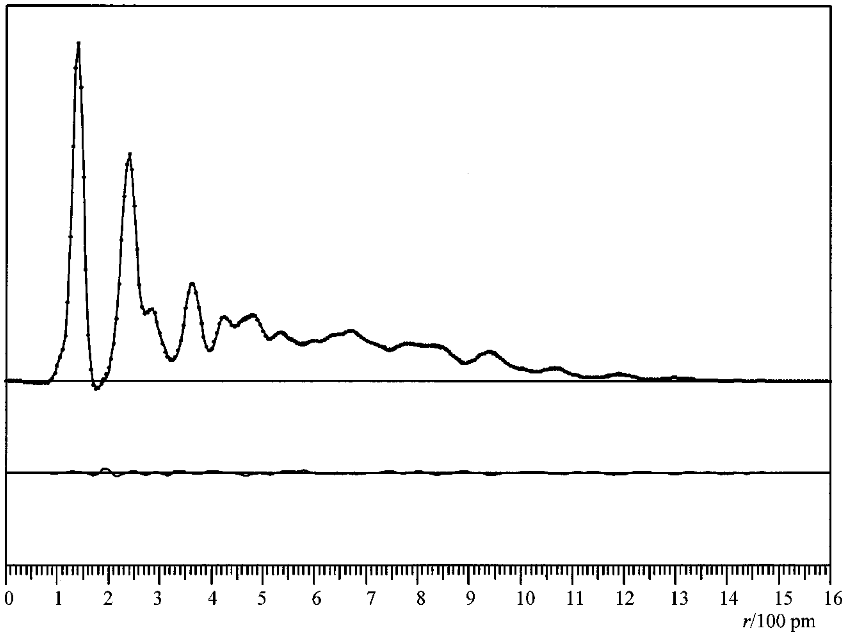

Figure 4. RD curves for the best model of H_2Pc. The experimental points (dots) are the average of the four curves shown in Figure 5, and theoretical points were used for the unobserved region $s < 17.50$ nm^{-1}. The damping coefficient for the RD function is 35 pm^2. The curve below is the difference curve.

intramolecular H-bonding), and corresponds to the concerted mechanism; see Tables S2 and S3 for the complete geometry. According to the B3LYP/6-311++G** calculations, the stepwise transition state barrier is 64.2 kJ/mol, TS (C_s, N1−H, N2···H), while the concerted transition state barrier is 95.8 kJ/mol, TS (C_{2h}, N4···H, N2···H), measured from the most stable *trans* isomer. This clearly shows that the stepwise mechanism is preferred for H_2Pc as well as for H_2P. The normal mode analysis suggests that the frequency number 155 in Supporting Information Table S3 with symmetry B_{3g}, and wavenumber 181 cm^{-1} corresponds to a simultaneous opening of the two opposite azamethine angles and closing of the other two azamethine angles of the inner cavity in a such way that the H57 comes close to N2 and H58 close to N4, thereby makeing it possible to switch between the two equivalent *trans* forms.

Molecular Vibrations and Flexibility. The infrared[24,51–58] and Raman[24,59] spectra of H_2Pc have been recorded by several research groups. The most comprehensive vibrational investigation of the vibrational spectrum of *trans* H_2Pc has been made by Zhang and co-workers[24] where the vibrational assignments of the infrared and Raman spectra have been discussed. Their assignments are based on scaled B3LYP/6-31G* frequencies and infrared and Raman intensities. Our similar calculations using B3LYP/6-311++G** confirm their results, and our results without scaling are given as Supporting Information (Table S3). To our knowledge, no vibrational coordinate analysis has been

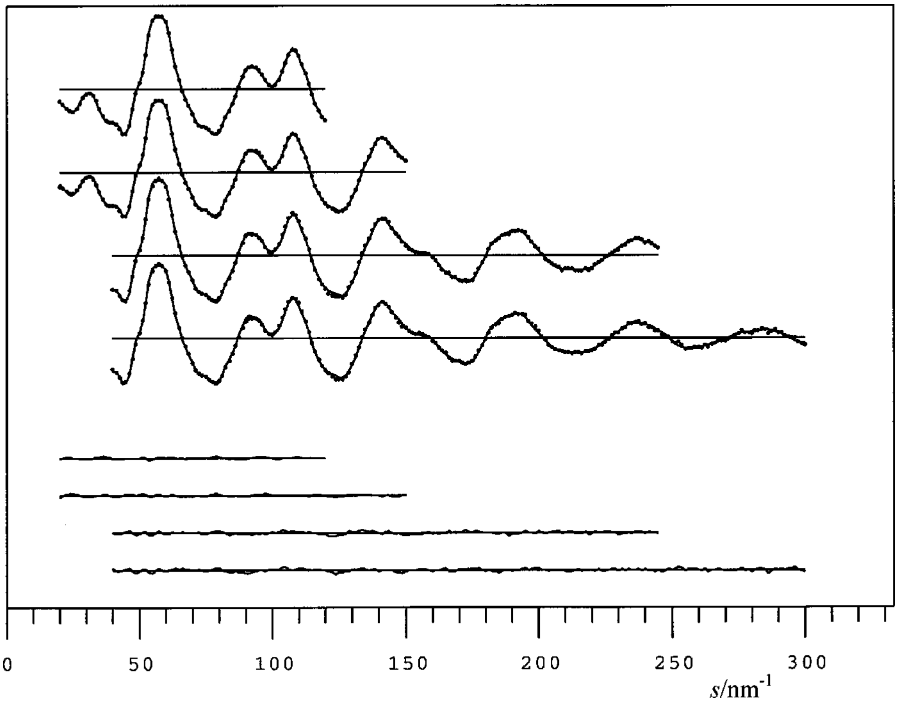

Figure 5. Average molecular intensity curves for the best model of H_2Pc. The first two curves are the average from eight sectors from the long camera distance along the *y*- and *x*-axis, respectively. The next two curves are the corresponding average curves from eight sectors from the middle camera distance. Dots are experimental points, and a full line is a theoretical curve. The four curves below are difference curves.

made for the *cis* isomer even if this is a stable isomer, but its existence has not been detected experimentally. Comparison of the vibrational frequencies in Table S3 for the two isomers shows that they all are very close to each other. Even if the intensities are different, it would be difficult to identify the *cis* isomer except for the N−H stretching frequencies, which are very different for the *trans* and *cis* isomers. The highest vibrational frequency is the symmetric N−H stretching, 3602 and 3323 cm^{-1}, for the *trans* and *cis* isomers, respectively. The asymmetric N−H stretching frequency is 3544 and 3274 cm^{-1}, and both of these frequencies are infrared active and well above the C−H stretching frequencies starting at about 3200 cm^{-1}. It should therefore be possible to detect the two N−H stretching vibrations of the *cis* isomer with infrared matrix spectroscopy and thereby get a confirmation of the existence of the *cis* isomer.

The MPcs have often been regarded as rigid molecules, but this is a rather doubtful description since six vibrational frequencies for the *trans* isomer are below 84 cm^{-1} according to the B3LYP/6-311++G** calculation. The five lowest vibrational frequencies for the *trans* isomer are all out-of-plane motions. The lowest motion (B_{3u}, 20 cm^{-1}) can best be described as the two opposite isoindole units moving up and the other two down. The next mode (B_{3u}, 38 cm^{-1}) is a breathing motion where all isoindole units are moving up or down, and the mode A_u (52 cm^{-1}) can be described as a twisting of the isoindole units as a propeller. The next two modes (B_{2g}, 55 cm^{-1}, and B_{1g}, 57 cm^{-1}) are similar where two opposite isoindole units are moving up or down and the other two isoindole units are twisting. The lowest in-plane motion (B_{3g}, 84 cm^{-1}) twists the isoindole units. With so many low vibrational modes, it is important to include the best available vibrational corrections terms in the GED analysis, and this was done using the curvilinear approach in the SHRINK program.

Experimental Structure. Because HF calculations are not able to describe the molecular ground-state structure neither for H_2P nor H_2Pc, how good are the B3LYP calculations? So far, the *cis* isomer has not been observed experimentally for H_2Pc, and there is only one investigation in the solid state that actually confirms that the two inner H atoms possess a *trans* configuration[12] in H_2Pc. A convenient way to test the quality of the quantum chemical calculations would be to directly compare the calculated equilibrium structures with the experimental data. The calculated equilibrium structures, Supporting Information Tables S1 and S2, and calculated u_{h1} values using the SHRINK program and the B3LYP/6-311++G** force field, were used to calculate the radial distribution (RD) curves for the *trans* and *cis* isomers, and these RD curves are shown in Figures 2 and 3, respectively. It should be mentioned that calculated geometry from the quantum chemical calculations refers to a r_e structure, while the experimental GED data represent a r_a structure, and that shrinkage has not been included. However, these effects are small and should therefore not significantly influence the agreement between theoretical and experimental data.

Comparison of the RD curves in Figures 2 and 3 shows that the agreement between calculated and experimental curves is significantly better for the *trans* isomer than for the *cis* isomer in the region 250−700 pm. This is mainly due to the difference of the azamethine N angles (see section 2, Table S2) for the *trans* and *cis* isomers. The GED data thus confirm the greater thermodynamic stability of the *trans* isomer and that the B3LYP/6-311++G** calculations are in very good agreement.

Assuming that there is a thermodynamic equilibrium between the two isomers at the recorded temperature of 471 °C, the mole fraction can be calculated from the relation: $\Delta G° = -RT\ln K$. A statistical weight of 2 and 4 is used for the *trans* and *cis* isomers, respectively. From the B3LYP/6-311++G** calculations, $\Delta E = 38.2$ kJ/mol, $\Delta G_{298}° = 34.9$ kJ/mol, and $\Delta G_{744}° = 33.2$ kJ/mol, assuming that the enthalpy and entropy differences are independent of the temperature. Because of these large values, the mole fraction of 99.8% of the *trans* isomer and only 0.2% of the *cis* isomer is obtained. It should be emphasized that the mole fraction of the *cis* isomer decreased to zero when refinement of structure parameters for the *trans* isomer was included; therefore, we have excluded the *cis* isomer in the final refinements.

In addition, attempts were made to refine the out-of-plane angle of the N1−H57 bond relative to the plane defined by the atoms C5, N1, and C6 to determine the position of inner hydrogen atoms. The out-of-plane angle for the N3−H58 bond is assumed to be moving in an opposite direction of the out-of-plane angle for the N1−H57 bond. Because of low scattering power of the H atoms, this out-of-plane angle cannot be accurately determined by the GED method, and these out-of-plane angles were therefore fixed to zero as predicted by all quantum chemical calculations.

The final experimental GED structure is presented in Table 2 together with the X-ray structure and the B3LYP/cc-VTZ structure. RD curves and intensity curves corresponding to this best model are shown in Figures 4 and 5, respectively.

The other GED structure parameters, not given in Table 2, can be obtained from the constraints given in the model and constraints section. Even if the structure parameters obtained from the different methods are not strictly comparable, the general agreement is very good, and the B3LYP calculations with basis sets of 6-311++G** and cc-pVTZ quality satisfactorily reproduce the experimental results. A more detailed comparison of the solid state and gas phase structure parameters is not justified since the uncertainties from the GED are underestimated due to the applied constraints and symmetry equivalent bond distances and bond angles in X-ray are more different than their quoted uncertainties. It should also be noted that all calculated bond lengths decreased by about 0.3 pm going from B3LYP/6-311++G** (grid = default) to B3LYP/cc-pVTZ (grid = ultrafine).

Concluding Remarks

H_2Pc is predicted to exist as two isomers by B3LYP calculations, a *trans* form (D_{2h}) and a *cis* form (C_{2v}), with the *trans* form about 40 kJ more stable than the *cis* form. In the gas phase, only the *trans* isomer is found. B3LYP force field calculations indicate that the unidentified *cis* form might be experimentally detected for the first time by infrared matrix spectroscopy because the N−H stretching frequencies are substantially different for the two forms. There is good agreement between the geometry obtained from B3LYP calculations, GED and X-ray. H_2Pc is a flexible molecule where the five lowest frequencies are all related to out-of-plane motion of the isoindole units. B3LYP calculations support that the NH tautomerization proceeds by a stepwise mechanism.

Acknowledgment. S. Gundersen is acknowledged for workup of the experimental data. The University of Oslo is thanked for a generous amount of computer time. T.S. thanks the International Student Quota Program of the University of Oslo for financial support.

Supporting Information Available: Selected interatomic distances (pm) for H_2Pc (Table S1), selected bond angles (degree) for H_2Pc (Table S2), and calculated vibrational frequencies (cm^{-1}), IR intensities (km/mol), and Raman intensities (Å^4/amu) for *trans* and *cis* isomers of H_2Pc (Table S3). This material is available free of charge via the Internet at http://pubs.acs.org.

References and Notes

(1) Kadish, K. M., Smith, K. M., Guilard, R., Eds. Application of phthalocyanines. *The Porphyrin Handbook*; Academic Press: San Diego, CA, 2003; Vol. 19.

(2) Kadish, K. M., Smith, K. M., Guilard, R., Eds. Phthalocyanines: Properties and materials. *The Porphyrin Handbook*; Academic Press: San Diego, CA, 2003; Vol. 17.

(3) Kadish, K. M., Smith, K. M., Guilard, R., Eds. Phthalocyanines: Spectroscopic and electrochemical characterization. *The Porphyrin Handbook*; Academic Press: San Diego, CA, 2003; Vol. 16.

(4) Engel, M. K. *The Porphyrin Handbook, Single-Crystal Structures of Phthalocyanine Complexes and Related Macrocycles*; Academic Press: San Diego, CA, 2003; Vol. 20.

(5) McKeown, N. B. *Phthalocyanine Materials: Structure, Synthesis and Function*; Cambridge University Press: Cambridge, 1998.

(6) Leznoff, C. C., Lever, A. B. P., Eds. *Phthalocyanines—Properties and Applications*; VCH Publishers: New York, 1989; Vol. 1; 1992, Vol. 2; 1993, Vol. 3; 1996, Vol. 4.

(7) Robertson, J. M. *J. Chem. Soc.* **1936**, 1195.

(8) Janczak, J.; Kubiak, R. *J. Alloys Compd.* **1992**, *190*, 121.

(9) Janczak, J. *Pol. J. Chem.* **2000**, *74*, 157.

(10) Hoskins, B. F.; Mason, S. A.; White, J. C. B. *J. Chem. Soc. D: Chem. Commun.* **1969**, 554.

(11) Kubiak, R.; Janczak, J. *J. Alloys Compd.* **1992**, *190*, 117.

(12) Matsumoto, S.; Matsuhama, K.; Mizuguchi, J. *Acta Crystallogr.* **1999**, *C55*, 131.

(13) Zugenmaier, P.; Bluhm, T. L.; Deslandes, Y.; Orts, W. J.; Hamer, G. K. *J. Mater. Sci.* **1997**, *32*, 5561.

(14) Engel, M. K. *Kawamura Rikagaku Kenkyusho Hokoku* **1997**, 11.

(15) Maity, D. K.; Truong, T. N. *J. Porphyrins Phthalocyanines* **2001**, *5*, 289.

(16) Ghosh, A.; Almloef, J. *J. Phys. Chem.* **1995**, *99*, 1073.

(17) Samdal, S.; Volden, H. V.; Ferro, V. R.; Garcia de la Vega, J. M.; Gonzalez-Rodriguez, D.; Torres, T. *J. Chem. Phys.* **2007**, *111*, 4542.

(18) Strenalyuk, T.; Samdal, S.; Volden, H. V. *J. Phys. Chem. A* **2007**, *111*, 12011.

(19) Frisch, M. J.; Trucks, G. W.; Schlegel, H. B.; Scuseria, G. E.; Robb, M. A.; Cheeseman, J. R.; Montgomery, J. A., Jr.; Vreven, T.; Kudin, K. N.; Burant, J. C.; Millam, J. M.; Iyengar, S. S.; Tomasi, J.; Barone, V.; Mennucci, B.; Cossi, M.; Scalmani, G.; Rega, N.; Petersson, G. A.; Nakatsuji, H.; Hada, M.; Ehara, M.; Toyota, K.; Fukuda, R.; Hasegawa, J.; Ishida, M.; Nakajima, T.; Honda, Y.; Kitao, O.; Nakai, H.; Klene, M.; Li, X.; Knox, J. E.; Hratchian, H. P.; Cross, J. B.; Adamo, C.; Jaramillo, J.; Gomperts, R.; Stratmann, R. E.; Yazyev, O.; Austin, A. J.; Cammi, R.; Pomelli, C.; Ochterski, J. W.; Ayala, P. Y.; Morokuma, K.; Voth, G. A.; Salvador, P.; Dannenberg, J. J.; Zakrzewski, V. G.; Dapprich, S.; Daniels, A. D.; Strain, M. C.; Farkas, O.; Malick, D. K.; Rabuck, A. D.; Raghavachari, K.; Foresman, J. B.; Ortiz, J. V.; Cui, Q.; Baboul, A. G.; Clifford, S.; Cioslowski, J.; Stefanov, B. B.; Liu, G.; Liashenko, A.; Piskorz, P.; Komaromi, I.; Martin, R. L.; Fox, D. J.; Keith, T.; Al-Laham, M. A.; Peng, C. Y.; Nanayakkara, A.; Challacombe, M.; Gill, P. M. W.; Johnson, B.; Chen, W.; Wong, M. W.; Gonzalez, C.; Pople, J. A. *Gaussian 03*, Revision B.03; Gaussian, Inc.: Pittsburgh, PA, 2003.

(20) Boronat, M.; Viruela, R.; Orti, E. *Synth. Met.* **1995**, *71*, 2291.

(21) Dent, G.; Farrell, F. *Spectrochim Acta, Part A* **1997**, *53A*, 21.

(22) Day, P. N.; Wang, Z.; Pachter, R. *THEOCHEM* **1998**, *455*, 33.

(23) Cortina, H.; Senent, M. L.; Smeyers, Y. G. *J. Phys. Chem. A* **2003**, *107*, 8968.

(24) Zhang, X.-X.; Bao, M.; Pan, N.; Zhang, Y.-X.; Jiang, J.-Z. *Chin. J. Chem.* **2004**, *22*, 325.

(25) Becke, A. D. *J. Chem. Phys.* **1993**, *98*, 5648.

(26) Lee, C.; Yang, W.; Parr, R. G. *Phys. Rev. B* **1988**, *37*, 785.

(27) Ferro, V. R.; Poveda, L. A.; Claessens, C. G.; Gonzalez-Jonte, R. H.; Garcia de la Vega, J. M. *Int. J. Quantum Chem.* **2003**, *91*, 369.

(28) Gong, X. D.; Xiao, H. M.; Gao, P.; Tian, H. *THEOCHEM* **2002**, *587*, 189.

(29) Ferro, V. R.; Garcia de la Vega, J. M.; Claessens, C. G.; Poveda, L. A.; Gonzalez-Jonte, R. H. *J. Porphyrins Phthalocyanines* **2001**, *5*, 491.

(30) Ferro, V. R.; Garcia de la Vega, J. M.; Gonzalez-Jonte, R. H.; Poveda, L. A. *THEOCHEM* **2001**, *537*, 223.

(31) Ryeng, H.; Ghosh, A. *J. Am. Chem. Soc.* **2002**, *124*, 8099.

(32) Vangberg, T.; Lie, R.; Ghosh, A. *J. Am. Chem. Soc.* **2002**, *124*, 8122.

(33) Wasbotten, I. H.; Wondimagegn, T.; Ghosh, A. *J. Am. Chem. Soc.* **2002**, *124*, 8104.

(34) Ghosh, A. *J. Porphyrins Phthalocyanines* **2000**, *4*, 380.

(35) Nguyen, K. A.; Pachter, R. *J. Phys. Chem A* **2000**, *104*, 4549.

(36) Parusel, A. B. J.; Ghosh, A. *J. Phys. Chem. A* **2000**, *104*, 2504.

(37) Parusel, A. B. J.; Wondimagegn, T.; Ghosh, A. *J. Am. Chem. Soc.* **2000**, *122*, 6371.

(38) Hariharan, P. C.; Pople, J. A. *Mol. Phys.* **1974**, *27*, 209.

(39) Krishnan, R.; Binkley, J. S.; Seeger, R.; Pople, J. A. *J. Chem. Phys.* **1980**, *72*, 650.

(40) Frisch, M. J.; Pople, J. A.; Binkley, J. S. *J. Chem. Phys.* **1984**, *80*, 3265.

(41) Dunning, T. H., Jr *J. Chem. Phys.* **1989**, *90*, 1007.

(42) Porezag, D.; Pederson, M. R. *Phys. Rev. B* **1996**, *54*, 7830.

(43) Halls, M. D.; Schlegel, H. B. *J. Chem. Phys.* **1998**, *109*, 10587.

(44) Johnson, B. G.; Florian, J. *Chem. Phys. Lett.* **1995**, *247*, 120.

(45) Halls, M. D.; Schlegel, H. B. *J. Chem. Phys.* **1999**, *111*, 8819.

(46) Sipachev, V. A. *THEOCHEM* **1985**, *22*, 143.

(47) Sipachev, V. A. *J. Mol. Struct.* **2001**, *567−568*, 67.

(48) Hedberg, L.; Mills, I. M. *J. Mol. Spectrosc.* **1993**, *160*, 117.

(49) Hedberg, L.; Mills, I. M. *J. Mol. Spectrosc.* **2000**, *203*, 82.

(50) Gundersen, G.; Samdal, S.; Seip, H.-M.; Strand, T. G. Annual Report 1977, 1980, 1981 from the Norwegian Gas Electron Diffraction Group.

(51) Cannon, C. G.; Sutherland, G. B. B. M. *Spectrochim. Acta* **1951**, *4*, 373.

(52) Shurvell, H. F.; Pinzuti, L. *Can. J. Chem.* **1966**, *44*, 125.

(53) Kobayashi, T.; Kurokawa, F.; Uyeda, N.; Suito, E. *Spectrochim. Acta* **1970**, *26*, 1305.

(54) Kobayashi, T. *Spectrochim. Acta* **1970**, *26*, 1313.

(55) Brach, P. J.; Grammatica, S. J.; Ossanna, O. A.; Weinberger, L. *J. Heterocycl. Chem.* **1970**, *7*, 1403.

(56) Sammes, M. P. *J. Chem. Soc., Perkin Trans. 2* **1972**, 160.

(57) Stymne, B.; Sauvage, F. X.; Wettermark, G. *Spectrochim. Acta, Part A* **1979**, *35A*, 1195.

(58) Clarisse, C.; Riou, M. T. *Inorg. Chim. Acta* **1987**, *130*, 139.

(59) Janczak, J. *Pol. J. Chem.* **1998**, *72*, 1871.

JP801284C